PHYSICAL REVIEW B **79**, 201406(R) (2009)

Chirality induced by surface strain studied using scanning tunneling microscopy

Laurent Guillemot and Kirill Bobrov
Laboratoire des Collisions Atomiques et Moléculaires (LCAM), CNRS UMR 8625, UPS-11, Bâtiment 351, Orsay F-91405, France and Université Paris-Sud, Orsay F-91405, France

(Received 19 January 2009; revised manuscript received 30 April 2009; published 27 May 2009)

We present a scanning tunneling microscopy study of a thermally annealed oxygen covered Cu(110) -(2×1)-O surface. The thermal annealing results in step bunching followed by formation of strained terraces. The mechanical strain causes local compression of the Cu lattice accompanied with reflection symmetry breaking as measured by comparative analysis of the atomically resolved topographies. On the strained terraces the oblique Cu lattice favors oxygen rearrangement into a chiral adsorption phase. Chiral surface organization is evidenced by formation of enantiomorphic domains on the strained terraces.

DOI: 10.1103/PhysRevB.79.201406 PACS number(s): 68.35.Gy, 68.37.Ef, 68.43.Fg, 68.43.Hn

Chirality is a property widespread in nature characterizing an object that cannot be superimposed with its mirror image. It follows that any chiral system can exist in two mirror image forms called enantiomers. Nowadays chiral solid surfaces are thought to provide a promising tool for either synthesis of pure enantiomers or to allow their identification and separation. Presence or creation of chirality on surfaces requires sufficient complexity so that any reflection symmetry in the system is absent or destroyed. High-Miller-index surfaces naturally provide chiral sites at specific surface locations such as steps or kinks.[1–5] On low-Miller-index surfaces, the most commonly used approach to create chirality is "chiral modification"[6–9] method which consists of adsorption of large chiral or prochiral organic molecules (acids,[10–13] aromatics,[14] and amino-acids[11,15,16]). Adsorption of such molecules can reveal two-dimensional (2D) chirality when the molecules are assembled on the surface into ordered arrays possessing no reflection symmetry.

In this Rapid Communication we will demonstrate a method to create chirality on an achiral low-Miller-index metallic surface. Specifically, we will show that mechanical stress, developed into the purely inorganic Cu(110)-O interface, introduces chirality into the oxygen adsorption phase. In this case complexity is provided by mechanical stress which deforms the Cu substrate, breaks its reflection symmetry, and modifies the adsorbate structure giving rise to surface chirality.

A single-crystal Cu(110) sample cut with maximal achievable accuracy of ~0.1° was used in this study. The thoroughly polished Cu(110) sample was cleaned *in situ* by repeated cycles of sputtering (1 keV Ar^+) at grazing incident angles followed by thermal annealing at 650 °C. Molecular oxygen adsorption was performed at ~220 °C by *in situ* exposing the Cu(110) surface to oxygen at $P=5\times10^{-10}$ mbar for ~15 min until ~0.25 ML oxygen coverage was reached on the surface. Cleanness of the prepared surface was controlled by Auger electron spectroscopy (AES) and scanning tunneling microscopy (STM); no impurities were detected. Then the surface was annealed at a temperature of 560 °C. After cooling down to room temperature STM topographies were recorded by tunneling from occupied states of the surface ($U_{bias}=-1.5$ V, $I_t=0.5$ nA). Topography distortion was then corrected using the known geometry of the Cu(110)-(2×1)-O adsorption phase as a reference.

The thermal annealing induces substantial modifications of the surface at mesoscopic scale visible on the STM topography (Fig. 1) as follows: (i) surface terrace ripening favors larger terraces forcing monoatomic steps to assembly into SBs; (ii) oxygen-induced step etching reveals oxygen decorated [001] terrace borders; and (iii) new surface terraces (A–K) are produced where the step bunches are slightly twisted (9° deviation in azimuth). Local strain emerges on the substrate during its cooling down when Cu adatoms thermally diffusing on corrugated areas are no longer able to follow the substrate morphology by building up flat nondeformed surface terraces. This corrugated morphology can be readily deduced from the STM topography shown in Fig. 1.

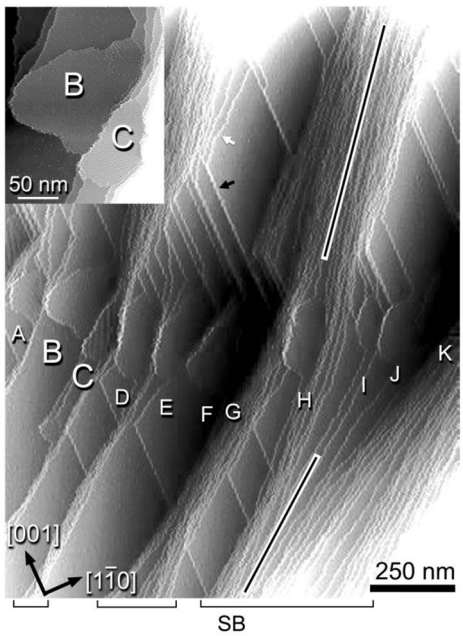

FIG. 1. Large scale STM topography of the Cu(110)-(2×1)-O surface. Surface steps—naturally existing and annealing produced—are marked by black and white arrows, respectively. Newly produced terraces are labeled as A–K. The black and white lines specify the azimuthal direction of the step bunches (SBs). In inset: magnified view on the B and C terraces.

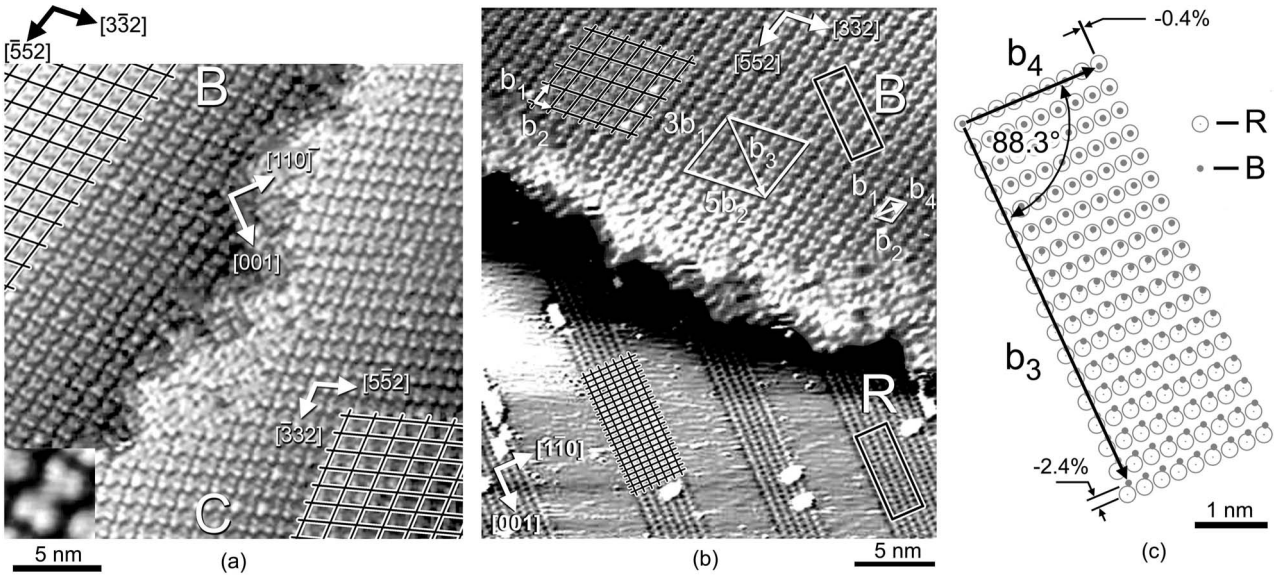

FIG. 2. Structure, symmetry, and stress of the new phase. (a) STM topography of the B and C terraces. Black and white lines show the symmetry grids; (b) STM topography of the interface between the (2×1)-O phase and B domain. Two 8×16 slabs of the Cu lattice, underlying domain B, and (2×1)-O phase (r) are shown as black and white rectangles. Construction of the B slab (b_3 and b_4 vectors) from the corresponding unit cell (b_1 and b_2 vectors) is shown schematically; (c) superposition of the (8×16) slabs. Compression of the Cu lattice underlying B domain is specified in percent.

In vicinity of the A–K terraces the step bunches are forced to deviate by ~9° in azimuth to follow slight mesoscopic variation[17] in the 0.1° sample miscut angle. The temperature decrease affects mobility of the step bunches which are also perturbed by emerging [001] terrace edges. The Cu adatoms precipitate into new terraces (A–K) which become laterally strained, accommodating the corrugated substrate morphology.

The striking observation is that afterwards Cu and O atoms stabilize on these strained terraces into a low-symmetry chiral phase which is drastically different from the well-known Cu(110)-(2×1):O strip phase.[18,19] In our previous study we found that local strain produced several oxygen adsorbate phases on the Cu(110)-O surface. Here we will consider one of them (labeled as A_2 in Ref. 20) in order to evaluate the role of surface strain in chiral organization on the surface. We will consider only B and C terraces (inset of Fig. 1) in detail, all other terraces were found to be equally strained and fully covered by the same oxygen adsorbtion phase.

STM topographies representing the adsorption phase covering B and C terraces as well as its interface with the (2×1)-O phase are shown in Figs. 2(a) and 2(b), respectively. This phase exists in the form of two enantiomorphic domains, B and C, covering entirely the corresponding terraces. The former structure has been already observed in our previous study.[20] Here, the STM topography of the B domain indicates butterflylike "tetramer" clusters ordered along the [$\bar{5}$52] and [3$\bar{3}$2] directions on the surface. Each "tetramer" cluster was found to consist of four CuO_2 fragments stabilized on the surface by the substrate strain. Here we report on the remarkable observation: the adsorption phase exists in the form of two distinguishable mirror domains. It can be readily seen that C domain consists of the same "tetramer" clusters but ordered along the [5$\bar{5}$2] and [$\bar{3}$32] directions which are mirror images of those of the B domain.

The "tetramer" units, being themselves enantiomers, appear to form chiral motifs on the surface. The chiral organization is manifested here by separate ordering of the enantiomers on large domains along two nonsymmetry directions on the surface. The enantiomorphic domains are always separated by terrace borders; no domain boundaries have been observed within the terraces.

The emerging chirality is a local property of the thermally annealed Cu(110)-O surface, the enantiomorphic domains are produced exclusively on the strained areas. The unstrained areas are covered by the well-known achiral (2×1):O strip phase. This strongly suggests that surface strain plays a crucial role in the chiral organization.

The well-established geometry of the (2×1)-O phase allows us to evaluate the strain of the Cu substrate underlying each enantiomorphic domain.[21] Perfectly orthogonal Cu lattice (R) was assumed for the (2×1)-O phase. Then we deduce the lattice underlying B domain using grid construction as detailed in Fig. 2(b). The superposition of the deduced lattices is shown in Fig. 2(c). The most striking observation is that stress, compressing the Cu substrate, breaks the lattice orthogonality. The angle (88.3°) between the [1$\bar{1}$0] and [001] vectors deviates slightly from its nominal value of 90° [Fig. 2(c)]. The same oblique unit cell was deduced for the Cu substrate underlying C domain, within the accuracy of the method. All the new terraces (A–K) were found to be equally strained and fully covered by this oxygen adsorption phase.

We attribute the chiral organization to the stress-induced compression of the substrate and, more specifically, to the breaking of orthogonality of the underlying Cu lattice. In this context it should be reminded that another adsorption phase [Cu(110)-$c(8\times2)$-O] was discovered in this system.[20] This

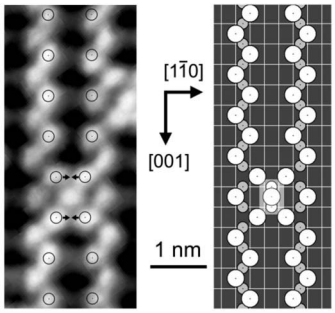

FIG. 3. STM topography of the (a) Cu(110)-$c(8\times2)$-O phase and its (b) structural model reproduced from Ref. 20. The arrows indicate symmetric approach of the four Cu atoms, belonging to the Cu-O chains (black circles), toward the isolated CuO_2 fragment located in the center [highlighted in (b)].

phase shown in Fig. 3 is produced on a compressed but orthogonal substrate. A noteworthy feature is that this situation produces an achiral reconstructed phase. It strongly suggests that the reflection symmetry breaking is a key factor in formation of the chiral adsorption phase observed in this study.

Figures 4(a) and 4(b) represent close views on the B and C enantiomorphic domains. Their structural models [Figs. 4(c) and 4(d)] illustrate the position and orientation of the CuO_2 fragments composing the "tetramers." The primal step toward creation of a chiral motif is formation of CuO_2 fragments instead of either straight or zig-zag Cu-O chains. This stage is directly related to the reflection symmetry breaking. Indeed, during heating and subsequent cooling down of the surface, the Cu and O atoms thermally diffusing on the strained terraces cannot assemble into continuous (2×1)-O chains as they do on the unstrained areas: the broken reflection symmetry makes the highly symmetric chains no longer stable. The Cu and O atoms precipitate on the substrate in the form of CuO_2 fragments [Figs. 4(c) and 4(d)]; their short length and lower symmetry allow the atoms to change their position more easily and to accommodate better the geometry of the deformed Cu lattice.

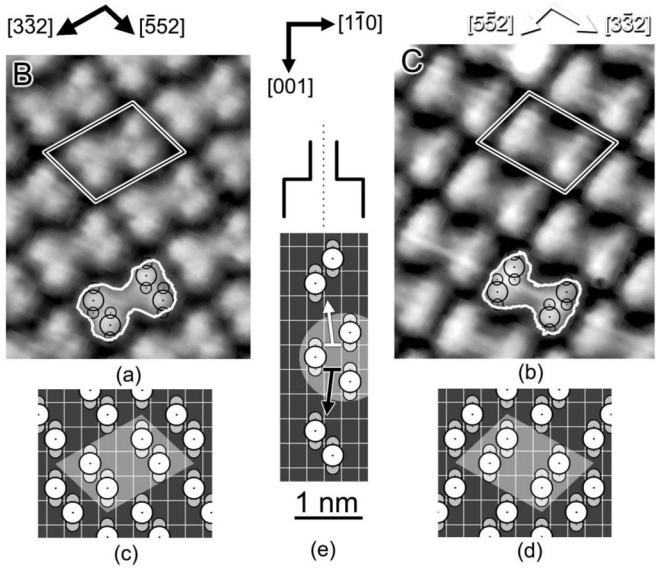

FIG. 4. Chiral organization on the strained Cu(110)-O surface. (a) and (b): STM topographies of the two enantiomorphic domains. The black and white lines specify the unit cell of each domain. The white contour lines depict the Cu_4O_8 "tetramer" units where Cu and O atoms are shown as large and small black circles, respectively. (c) and (d) Structural models of the enantiomorphic domains shown in (a) and (b). Cu and O atoms are shown as white and gray circles, respectively. The unit cells of both domains are highlighted; the close-packed rows of the Cu substrate are shown as white grid lines. (e) Schematics of the CuO_2 fragments pairing. The arrows designate pairing of the single CuO_2 fragments (highlighted) into two mirror forms of the Cu_2O_4 dimmers.

Furthermore, the atomically resolved structure of the "tetramer" units suggests pairing of the CuO_2 fragments. Each lobe of the butterflylike units in Figs. 4(a) and 4(b) consists of two paired CuO_2 fragments. These Cu_2O_4 dimmers, having characteristic "kinked" structure as shown in Fig. 4(e), are the smallest units within which chirality first emerges. Obviously, formation of the Cu_2O_4 dimmers requires short-range lateral attractive interaction to be formed. Figure 3 provides experimental evidence for the existence of this attractive force. The CuO_2 fragment, occasionally present between the $c(8\times2)$-O chains,[20] induces lateral approach of the four nearest Cu atoms surrounding the fragment.

Creation of chiral motif is a well-known phenomenon which usually takes place upon adsorption of either intrinsically chiral or prochiral molecules, which lose all their reflection symmetry planes by bonding to the surface. The phenomenon presented in this study is qualitatively different from that previously reported.[22] Here chirality first emerges as a result of autoassembly of intrinsically achiral "molecules" (CuO_2 fragments) into chiral motifs and then propagates on the surface by assembling the chiral motifs into ordered domains.

In general the structure of molecule self-assemblies on metal surfaces is driven by a balance between metal-molecule interaction and intermolecular interactions. In the present case formation of the chiral domains arises from strong oxygen-metal interaction which defines adsorption sites for the CuO_2 fragments, combined with intermolecular surface-mediated interaction between the Cu_2O_4 dimmers. This latter interaction is manifested in the STM topographies as anisotropic modulation of the surface electronic density along specific directions, displaying the butterflylike shapes that can be viewed as a "coupling" of the Cu_2O_4 dimmers into "tetramer" units [Figs. 4(a) and 4(b)]. In the absence of lateral interaction, the Cu_2O_4 dimmers would appear as equally spaced identical units. This obviously is not the case. The highly anisotropic surface-mediated interaction favors dimmer alignment in either the $[3\bar{3}2]$ or $[\bar{3}32]$ direction depending on the actual domain [Figs. 4(a) and 4(b)]. It introduces unbalance into the CuO_2 fragments pairing since only one enantiomer can be aligned for a given direction. Therefore, only "enantioselected" Cu_2O_4 dimmers line up in a given direction and further assemble into 2D homochiral domains. Since the alignment is equally possible in two $[3\bar{3}2]$ and $[\bar{3}32]$ directions on the surface, two enantiomorphic $[-5\ 2\ 3\ 2]$ and $[5\ 2\ -3\ 2]$ domains are produced.

In conclusion, we have shown a way to chiral organization of achiral molecules on a metal surface. We anticipate that the observed strain-induced symmetry breaking is a common phenomenon for other adsorbate-metal systems. We expect that the formation of enantiomorphic domains on the strained Cu(110)-O surface, studied here at the atomic scale using STM, will shed light on the way chiral structures emerge on surfaces and how chiral information propagates over them. This method provides a "nanoscale laboratory" that opens perspective to better understand at the atomic scale the role of chirality in different surface related processes.

[1] D. S. Sholl, A. Asthagiri, and T. D. Power, J. Phys. Chem. B **105**, 4771 (2001).
[2] Y. Huang and A. J. Gellman, Catal. Lett. **125**, 177 (2008).
[3] C. F. McFadden, P. S. Cremer, and A. J. Gellman, Langmuir **12**, 2483 (1996).
[4] A. Ahmadi, G. Attard, J. Feliu, and A. Rodes, Langmuir **15**, 2420 (1999).
[5] J. D. Horvath and A. J. Gellman, J. Am. Chem. Soc. **123**, 7953 (2001).
[6] S. M. Barlow and R. Raval, Surf. Sci. Rep. **50**, 201 (2003).
[7] S. De Feyter and F. C. De Schryver, Chem. Soc. Rev. **32**, 139 (2003).
[8] R. Raval, Curr. Opin. Solid State Mater. Sci. **7**, 67 (2003).
[9] V. Humblot, S. M. Barlow, and R. Raval, Prog. Surf. Sci. **76**, 1 (2004).
[10] V. Humblot, M. Ortega Lorenzo, C. J. Baddeley, S. Haq, and R. Raval, J. Am. Chem. Soc. **126**, 6460 (2004).
[11] M. Ortega Lorenzo, C. J. Baddeley, C. Muryn, and R. Raval, Nature (London) **404**, 376 (2000).
[12] S. De Feyter, A. Gesquière, P. C. M. Grim, F. C. De Schryver, S. Valiyaveettil, C. Meiners, M. Sieffert, and K. Müllen, Langmuir **15**, 2817 (1999).
[13] F. Vidal, E. Delvigne, S. Stepanow, N. Lin, J. V. Barth, and K. Kern, J. Am. Chem. Soc. **127**, 10101 (2005).
[14] R. Fasel, M. Parschau, and K. H. Ernst, Nature (London) **439**, 449 (2006).
[15] E. Mateo Marti, S. M. Barlow, S. Haq, and R. Raval, Surf. Sci. **501**, 191 (2002).
[16] Q. Chen, D. J. Frankel, and N. V. Richardson, Surf. Sci. **497**, 37 (2002).
[17] N. Reinecke, S. Reiter, S. Vetter, and E. Taglauer, Appl. Phys. A **A75**, 1 (2002).
[18] F. Jensen, F. Besenbacher, E. Laegsgaard, and I. Stensgaard, Phys. Rev. B **41**, 10233 (1990).
[19] K. Kern, H. Niehus, A. Schatz, P. Zeppenfeld, J. Goerge, and G. Comsa, Phys. Rev. Lett. **67**, 855 (1991).
[20] K. Bobrov and L. Guillemot, Phys. Rev. B **78**, 121408(R) (2008).
[21] M. Aketagawa and K. Takada, Nanotechnology **6**, 105 (1995).
[22] V. Humblot and R. Raval, Appl. Surf. Sci. **241**, 150 (2005).